PHYSICAL REVIEW B VOLUME 25, NUMBER 7 1 APRIL 1982

# The Kondo problem. I. Transformation of the model and its renormalization

P. Schlottmann
*Institut für Theoretische Physik, Freie Univeristät Berlin, Arnimallee 3, 1000 Berlin 33, Germany*
(Received 22 September 1980)

A magnetic (spin-$\frac{1}{2}$) impurity in a metal shows a crossover from the asymptotically free spin at high temperatures to a singlet state at low temperatures. The susceptibility and the impurity lifetime are finite at zero temperature since the magnetic moment of the impurity is compensated by the conduction electrons. The qualitative change from infinite (free impurity spin) to a finite lifetime or susceptibility at $T=0$ represents a symmetry breaking which cannot be achieved by perturbation theory. We transform the *s-d* Hamiltonian such that the renormalization can be started with a finite relaxation time. The transformed Hamiltonian consists of a resonance level (the Toulouse limit) and a large perturbation. The resonance width acts like an infrared cutoff such that perturbation expansion at $T=0$ converges term by term. We show that the transformed Hamiltonian obeys multiplicative renormalization in leading and next-leading logarithmic order and derive the scaling laws of this system.

## I. INTRODUCTION

The Kondo problem[1,2] consists of a magnetic impurity, idealized by a spin $\frac{1}{2}$, coupled to an electron gas via an exchange interaction $J$. In the absence of a magnetic field the scattering of conduction electrons off the impurity causes electron-hole excitations with arbitrarily small energies. These excitations reflect in logarithmic infrared divergences at low temperatures owing to the sharp edge of the Fermi-Dirac distribution. The main problem then consists in removing these logarithmic divergences at low temperatures.

At high temperatures, $T>>T_K$ ($T_K$ being the Kondo temperature), the impurity is only weakly coupled to the electron gas and the system behaves essentially like a free spin. At low temperatures, $T<<T_K$, and for antiferromagnetic coupling the impurity spin is strongly coupled to the metal as a consequence of the infrared singularities.[3] The impurity spin and the conduction-electron-spin density form a singlet state and the system is nonmagnetic. For temperatures around $T_K$ there is a crossover between these two qualitative distinct situations. So far, there is no simple physical picture to describe the crossover region. It is Wilson's[4] main achievement to link numerically the weak and strong coupling regimes.

The Kondo problem is then a hard, although manageable example for a crossover between infrared slavery and asymptotic freedom. Moreover, the Kondo problem is experimentally accessible over the full range from weak to strong coupling. A typical example is the dilute alloy Fe*Cu*.[5-9]

Another important feature of the Kondo problem is its universal scaling behavior[3,4] for the small bare coupling constant $J$. The properties of the model only depend on the energy scale $T_K$ and are essentially independent on the choice of the density of states for the conduction electrons. It is usual to classify the perturbation expansion for any quantity by the hierarchy of the logarithmic divergences.[10] The leading and the next-leading logarithmic order, e.g., for the invariant coupling, determine the energy scale $T_K$.

Recently the Bethe ansatz has been successfully applied to the Kondo problem.[11,12] The method assumes that the $N$-body wave function factorizes into products of two-particle wave functions. It provides the exact static susceptibility and specific heat for all temperatures.[13,14] The Bethe ansatz, as well as Wilson's renormalization[4] are nonperturbative (in $J\rho$) strong-coupling approaches which express the result in terms of a (strong coupling) Kondo temperature with a renormalized band cutoff $\tilde{D}(J\rho)$. It is also possible to link the high- and low-temperature regimes by means of the traditional scaling approach. In this way we make use of perturbation theory and express the results in terms of the (weak coupling) Kondo temperature with the

 

bare band cutoff $D$. This, we believe, is the first successful attempt in this direction.

There is a close relation between the impurity-spin relaxation rate $1/T_1$ and the susceptibility.[15,16] A quenching of the magnetic moment at zero temperature is only possible if the impurity has a nonvanishing relaxation rate and vice versa. Hence the impurity spin has a relaxation rate of the order of $T_K$ at low temperatures. The free-impurity propagator is not a convenient basis to evaluate a physical quantity, since the perturbation theory diverges term by term. A finite-impurity lifetime, however, would provide a natural cutoff to the infrared singularities.[17,18] In this way, the relaxation rate plays a similar role as a "massive term" in quantum field theory or as the order parameter in phase transitions. In the latter case the order parameter regularizes the otherwise divergent high-temperature expansion. Since a single impurity cannot undergo a phase transition at $T_K$, there is a continuous crossover from the singlet state at low temperatures to a free-impurity spin at high temperatures.

The inclusion of a nonzero relaxation rate at low temperatures corresponds to a symmetry breaking from a stable spin with infinite lifetime, to a relaxing spin with finite lifetime. The zero-temperature relaxation rate is proportional to the Knodo temperature and hence a nonanalytic function of the coupling constant, and cannot be obtained by ordinary perturbative methods. It is therefore necessary to transform the Kondo Hamiltonian in order to create a massive term. Such a massive term can be thought of as a hybridization of the impurity spin with new pseudofermions,[19,20] such that the system then consists of a resonant level and a perturbation.[17,18]

The resonance width now provides the desired infrared cutoff and the perturbation expansion does not diverge term by term. The renormalization group and the solution of the x-ray-threshold problem are useful tools for a consistent treatment of the perturbation. The essential point is a careful renormalization of the resonance width. With the knowledge of the renormalized resonance width it is possible to obtain the susceptibility and the relaxation rate as shown in the following papers. Both have the correct Fermi-liquid behavior at low temperatures[21,22] and reproduce the perturbation theory at high temperatures.

The finite lifetime prevents the effective invariant-coupling $J$ to diverge. Moreover, the renormalized invariant coupling remains smaller than one for all energies and a consistent perturbation expansion according to the logarithmical hierarchy converges.

The rest of the paper is organized as follows. In Sec. II we briefly discuss the transformation of the $s$-$d$ model which leads to the explicit massive term. The method of bosonization of fermions is used to change the spin-flip excitations of the conduction electrons from bosonlike to fermionlike. In Sec. III we show that the transformed Hamiltonian obeys multiplicative renormalization in leading and next-leading logarithmic order. We derive scaling equations explicity for the four-leg vertex, the two-leg vertex, the impurity propagator, and the hybridization response function. In Sec. IV we rederive the results using the renormalization group method. In Sec. V we discuss the analogy of the model with the x-ray-threshold problem and use this analogy to generalize the scaling equations to nonzero temperature and to fix multiplicative constants. Some concluding remarks follow in Sec. VI.

In the following papers we first give a simple qualitative solution of the above-mentioned scaling equations. This simple solution already yields the correct crossover from the asymptotic freedom to infrared slavery. It reproduces the perturbation expansion up to third order in $J$ at high temperatures and shows Fermi-liquid properties at low temperatures. The susceptibility and the relaxation rate are in qualitative and quantitative agreement with our previous results.[15,16] Owing to the preferential treatment of $J_{||}$ with respect to $J_{\perp}$, the simple solution does not have the correct energy scale. This drawback is corrected with the sophisticated solution of the scaling equations. The results are compared with Wilson's numerical diagonalization of the Kondo Hamiltonian[4] and with the Monte Carlo calculation by Schotte and Schotte.[23]

## II. TRANSFORMATION OF THE $s$-$d$ HAMILTONIAN

In this section we briefly review the transformation of the $s$-$d$ model into a resonant level. Since we already presented this transformation in some detail,[17,18,24] we are only going to sketch the main points.

The $s$-$d$ model is given by

$$H=\sum_{\vec{k}\sigma}\epsilon_k c^{\dagger}_{\vec{k}\sigma}c_{\vec{k}\sigma}-BS_z + J\sum_{\vec{k}\vec{k}'\sigma\sigma'} S\cdot s_{\sigma\sigma'}c^{\dagger}_{\vec{k}\sigma}c_{\vec{k}'\sigma'}\ , \tag{2.1}$$

where $B$ is the Zeeman energy and $c^{\dagger}_{\vec{k}\sigma}$ is the creation operator for an electron with momentum $\vec{k}$ and spin $\sigma$. The exchange constant $J$ is positive for antiferromagnetic coupling between impurity and electrons, and negative for ferromagnetic coupling.

We replace the impurity-spin operators by fermion operators

$$S^{+}\leftrightarrow d^{+},\ S^{-}\leftrightarrow d,\ \text{and}\ S_z\leftrightarrow d^{\dagger}d-\tfrac{1}{2}\ . \tag{2.2}$$

The conduction-electron operators are replaced by

$$b^{\dagger}_{k\sigma}=\frac{1}{\sqrt{k}}\sum_{p=0}^{k_0}c^{\dagger}_{p+k\sigma}c_{p\sigma},\ b_{k\sigma}=b^{\dagger}_{-k\sigma} \tag{2.3}$$

which obey boson commutation relations for low-lying excitations.[25] The bosons describe the electron-hole excitations of the electron gas. Here $k_0$ is a cutoff for the electronic excitations. The conduction-electron kinetic energy and the spin-non-flip interaction can be expressed with (2.3) in terms of boson operators. In order to transform the spin-flip interaction we make use of the boson representation of fermions[26]:

$$c_{\sigma}=\sqrt{k_0}\exp\left[-\sum_{k>0}\frac{1}{\sqrt{k}}(b^{\dagger}_{k\sigma}-b_{k\sigma})\right]. \tag{2.4}$$

It is convenient to introduce the operators

$$a_k=\frac{1}{\sqrt{2}}(b_{k\uparrow}-b_{k\downarrow}),\ f_k=\frac{1}{\sqrt{2}}(b_{k\uparrow}+b_{k\downarrow}) \tag{2.5}$$

which correspond to spin-density and charge-density excitations of the electron gas, respectively. Since the $s$-$d$ interaction depends only on the spin-density operators, the charge distribution is not distorted. The charge-density excitations decouple from the spin-density excitations and can be separated from the problem.

The next step consists in applying the transformation[18,24,26]

$$U=\exp\left[(1-\sqrt{2})(d^{\dagger}d-\tfrac{1}{2})\sum_{k>0}\frac{1}{\sqrt{k}}(a^{\dagger}_k-a_k)\right] \tag{2.6}$$

to the system. This transformation changes the internal dimension of the spin-flip Hamiltonian from bilinear in conduction-electron operators (i.e., bosonlike) to linear in new pseudofermion operators. The new fermion operators are built up by the spin-density excitations and are defined by (2.4) with the $b^{\dagger}_{k\sigma}$ replaced by $a^{\dagger}_{k\sigma}$. A relation similar to (2.3) defines the $a_k$ in terms of the new fermion operators.

The Hamiltonian expressed in terms of the new fermion operators $c_k$, is now given by [17,18]

$$H=\sum_k\epsilon_k c^{\dagger}_k c_k-B(d^{\dagger}d-\tfrac{1}{2})+\tfrac{1}{2}J_{\perp}(d^{\dagger}c+c^{\dagger}d)$$
$$-\frac{1}{\rho}(\sqrt{2}-1-J_{\parallel}\rho/\sqrt{2})(d^{\dagger}d-\tfrac{1}{2})(c^{\dagger}c-\tfrac{1}{2})\ , \tag{2.7}$$

where $c^{\dagger}=\sum_k c^{\dagger}_k$ is the Wannier state at the impurity site. The first three terms describe a resonance level with resonance width $\Delta=(\pi/4)J^2_{\perp}\rho$. It corresponds to the "Toulouse limit" of the Kondo problem,[19,20] which is reached for $J_{\parallel}\rho=2-\sqrt{2}$.

We are going to call $\gamma\rho=\sqrt{2}-1-J_{\parallel}\rho/\sqrt{2}$ and analyze the perturbation theory with respect to $\gamma$ in the next section. As mentioned above, the hybridization $J_{\perp}$ acts like an infrared cutoff and prevents the perturbation expansion to diverge term by term.[17,18] The equivalence of the partition function of the models (2.1) and (2.7) has been shown independently by Vigman and Finkel'stein.[27] Our proof presented in Refs. 17 and 18, however, is more general since it identifies operators such that correlation functions also can be calculated. Both proofs are valid within the long-time approximation only.

## III. SCALING EQUATIONS OF THE TRANSFORMED MODEL

We discuss in this section the renormalization of physical quantities in leading and next-leading logarithmic order. The scaling equations are derived diagramatically using the Abrikosov-Sudakov method.[28,29]

### A. Renormalization of the four-leg vertex

Let $\Gamma$ be the four-leg and $V$ the two-leg vertex functions. The $d$-fermion (impurity spin) propagator can be written as

$$G_d(\omega)=d(\omega)/\{\,i[\omega+\Omega(\omega)\mathrm{sgn}\omega]\,\}\ , \tag{3.1}$$

where $\Omega(\omega)$ is the effective renormalized resonance width given by

$$\Omega(\omega)=\pi\rho_F V^2(\omega)d(\omega) \tag{3.2}$$

and $d(\omega)$ is a multiplicative renormalization factor

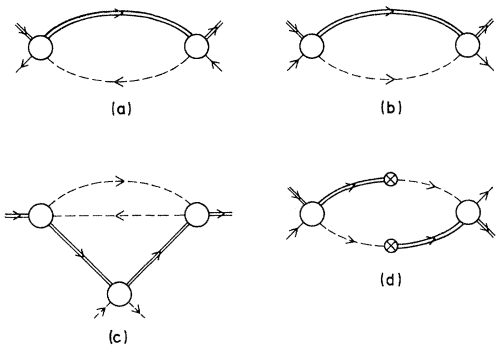


FIG. 1. Diagrams contributing in leading and next-leading logarithmic order to the four-leg vertex. The dashed lines represent the $c$-fermion propagator, the double full line a dressed impurity propagator, the circles correspond to a four-leg vertex depending on a single energy variable, and the encircled cross denotes a two-leg vertex. Here the Sudakov trick has been applied. The diagrams (a) and (b) contribute in leading order; they correspond to the zero sound and Cooper channels, respectively; (c) contributes to next-leading logarithmic order and (d) yields a nonlogarithmical correction for small $\gamma\rho$.

defined by (3.1). The self-energy of the $c$ fermions can be neglected.

The four-leg vertex depends, in principle, on three external energy variables. We have to consider two scattering channels known as the zero sound and Cooper channels[29,30] and to define irreducible vertex blocks within these channels in order to set up the parquet equations.[29,30] The parquet equations are a set of coupled integral equations whose solution yields the vertex function as a function of the three energy variables. This procedure is very tedious and can be avoided using the Sudakov method.[28–31] Here only one energy variable is considered and all irreducible vertex functions are replaced by a full vertex function. The external energy is to be taken smaller then the internal energies.

The leading logarithmic vertex diagrams are generated by the diagrams shown in Figs. 1(a) and 1(b). The dashed line represents a $c$-fermion propagator, the double full line a dressed-impurity propagator given by Eq. (3.1), and the circles the full one-energy four-leg vertex. The contribution of the diagram in Fig. 1(a) is given by

$$\gamma^2\rho\int_{|\omega|}^{D}d\omega'\frac{d(\omega')}{\omega'+\Omega(\omega')}\Gamma^2(\omega') \tag{3.3}$$

and it is easily seen that the diagram in Fig. 1(b) yields the same result with opposite sign. Hence the diagrams cancel each other and there are no vertex corrections in leading logarithmic order.[24,32]

Next-leading logarithmic contributions are generated by the diagram shown in Fig. 1(c). In the logarithmic approximation we have

$$\gamma^3\int_{|\omega|}^{D}d\omega'\left[\frac{d(\omega')}{\omega'+\Omega(\omega')}\right]^2\Gamma^3(\omega')\chi(\omega')\ , \tag{3.4}$$

where $\chi(\omega)$ is the energy-dependent part of the susceptibility of the extended states, represented by the bubble of dashed lines in Fig. 1(c). There is a further diagram contributing to the four-leg vertex shown in Fig. 1(d) where the two-leg vertex is represented by a cross. Within the logarithmic approximation we obtain

$$-\gamma^2\rho\int_{|\omega|}^{D}d\omega'\left[\frac{d(\omega')}{\omega'+\Omega(\omega')}\Gamma(\omega')\right]^2\pi\rho_F V^2(\omega')\ . \tag{3.5}$$

It is easily seen that the second-order contribution in $\gamma$ is constant as $\omega\to 0$ and that the third-order terms are nondivergent. The contributions from this diagram are therefore not important for small $\gamma$ and will be neglected at this point.

In summary, the only relevant contribution to $\Gamma$ comes from Eq. (3.4). This defines an integral equation which can be reduced to a differential equation, since the dependence of (3.4) on $\omega$ is only via the integration limit

$$\frac{d\Gamma(\omega)}{d|\omega|}=\gamma^2\chi(\omega)\Gamma^3(\omega)\left[\frac{d(\omega)}{|\omega|+\Omega(\omega)}\right]^2\ . \tag{3.6}$$

In the absence of $J_\perp$ the energy-dependent part of $\chi(\omega)$ is given by $-\rho^2|\omega|$. For a resonant level ($J_\perp\neq 0$) the density of the extended states at the impurity site vanishes at the Fermi level and is small in an energy interval $\Omega$ around the Fermi level. Hence $\chi(\omega)$ is to be replaced by $-\rho^2[|\omega|+\Omega(\omega)]$ and

$$\frac{d\Gamma(\omega)}{d|\omega|}=-(\gamma\rho)^2\Gamma^3(\omega)\frac{d^2(\omega)}{|\omega|+\Omega(\omega)}\ . \tag{3.7}$$

### B. Renormalization of the impurity propagator

The self-energy diagram which leads to the renormalization of $d(\omega)$ is shown in Fig. 2. Here we

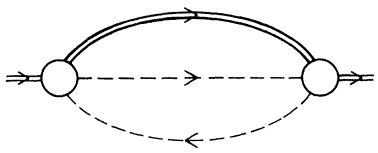

FIG. 2. Self-energy diagram for the impurity propagator as given by the Sudakov method.

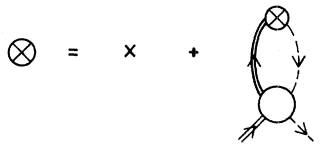

FIG. 3. Integral equation determining the two-leg vertex.

again used the Sudakov method. Within the logarithmic approximation we have

$$\Sigma(\omega)\simeq -i[\omega+\Omega(\omega)\mathrm{sgn}(\omega)](\gamma\rho)^2 \times\int_{|\omega|}^{D} d\omega'\Gamma^2(\omega')\frac{d(\omega')}{|\omega|+\Omega(\omega)} \tag{3.8}$$

and using the definition of $d(\omega)$, Eq. (3.1), we obtain

$$d(\omega)\simeq\left[1+(\gamma\rho)^2\int_{|\omega|}^{D} d\omega'\Gamma^2(\omega')\frac{d(\omega')}{\omega'+\Omega(\omega')}\right]^{-1} . \tag{3.9}$$

Again the variable $\omega$ appears only as the integration limit in the right-hand side (rhs) of (3.9) and the integral equations can be transformed into a differential equation

$$\frac{d\,d(\omega)}{d\,|\omega|}=(\gamma\rho)^2\Gamma^2(\omega)\frac{d^3(\omega)}{|\omega|+\Omega(\omega)} . \tag{3.10}$$

Both (3.7) and (3.10) generate next-leading logarithmic terms which contribute to the invariant coupling associated with the four-leg vertex. The invariant coupling is determined from the renormalization of the product $\Gamma(\omega)d(\omega)$. From (3.7) and (3.10) we have that

$$\frac{d}{d\,|\omega|}\Gamma(\omega)d(\omega)=d(\omega)\frac{d\Gamma(\omega)}{d\,|\omega|} +\Gamma(\omega)\frac{d\,d(\omega)}{d\,|\omega|}=0 \tag{3.11}$$

such that the invariant coupling is not renormalized, i.e., it remains equal to its bare value. This is the consequence of the Ward cancellation between vertex and self-energy diagrams.

### C. Renormalization of the two-leg vertex

In Fig. 3 we show schematically the integral equation determining the two-leg vertex. The bare vertex ($\frac{1}{2}J_\perp$) is denoted by a cross and the dressed vertex by an encircled cross. The integral equation reads within the logarithmic approximation

$$V(\omega)=\tfrac{1}{2}J_\perp-\gamma\rho\int_{|\omega|}^{D} d\omega' V(\omega')\Gamma(\omega')\frac{d(\omega')}{\omega'+\Omega(\omega')} . \tag{3.12}$$

Here we neglected the reduction of the $c$-fermion density of states for a resonant level close to the Fermi energy. Taking derivative with respect to $|\omega|$ we obtain the following differential equation:

$$\frac{dV(\omega)}{d\,|\omega|}=\gamma\rho\frac{V(\omega)}{|\omega|+\Omega(\omega)} , \tag{3.13}$$

where we have used the fact that $d(\omega)\Gamma(\omega)$ is constant and equal to one up to next-leading order.

The renormalized resonance width $\Omega$ can be obtained by means of Eqs. (3.2), (3.10), and (3.13). We have that

$$\frac{d\Omega(\omega)}{d\,|\omega|}=\pi\rho\frac{dV^2(\omega)}{d\,|\omega|}d(\omega)+\pi\rho V^2(\omega)\frac{d\,d(\omega)}{d\,|\omega|} =2\gamma\rho(1+\tfrac{1}{2}\gamma\rho)\frac{\Omega(\omega)}{|\omega|+\Omega(\omega)} . \tag{3.14}$$

The integration of this equation with the initial condition

$$\Omega(\omega=D)=\frac{\pi}{4}(J_\perp\rho)^2D \tag{3.15}$$

yields the effective resonance width at zero temperature as a function of energy and for small $\gamma\rho$.

### D. Renormalization of the hybridization response function

The hybridization response function is proportional to the correlation function

$$F(\omega)=-\pi\frac{J_\perp^2}{4}\langle\langle c^\dagger d;d^\dagger c\rangle\rangle_\omega ; \tag{3.16}$$

it describes the response of the effective hybridization (two-leg vertex) with respect to a small change in the hybridization. The bare correlation function is given by

$$F_0(\omega)=\pi\frac{J_\perp^2\rho}{4}\int_{|\omega|}^{D}d\omega'\frac{d(\omega')}{\omega'+\Omega(\omega')}\ , \tag{3.17}$$

where the reduction of the $c$-fermion density of states near the Fermi level is neglected.

$F(\omega)$ is diagramatically represented in Fig. 4(a). Since the Sudakov method[28–31] cannot be used directly for this quantity (it does not renormalize multiplicatively), we have to consider the four-leg vertex as a function of three energy variables. In order to reduce the problem to a single energy variable vertex we follow the procedure for the x-ray-threshold absorption spectrum $\chi$ in Ref. 30 and the density response function $D$ in Ref. 31 for an interacting electron gas in a strong magnetic field. We define

$$\Lambda=-[\,|\omega|+\Omega(\omega)]\frac{dF(\omega)}{d|\omega|} \tag{3.18}$$

and neglect the energy dependence of the $c$-fermion density of states. In analogy to Eqs. (3.29) and (3.31) in Ref. 31, the function $\Lambda$ then satisfies in the leading logarithmic approximation

$$\Lambda(\omega)=\frac{\pi}{4}J_\perp^2\rho\exp\left[-2\gamma\rho\int_{|\omega|}^{D}d\omega'\frac{d(\omega)\Gamma(\omega)}{|\omega|+\Omega(\omega)}\right].$$

If we also include the next-leading logarithms and differentiate we arrive at

$$\frac{d\Lambda(\omega)}{d|\omega|}=2\gamma\rho(1+\tfrac{1}{2}\gamma\rho)\frac{\Lambda(\omega)}{|\omega|+\Omega(\omega)}\ . \tag{3.19}$$

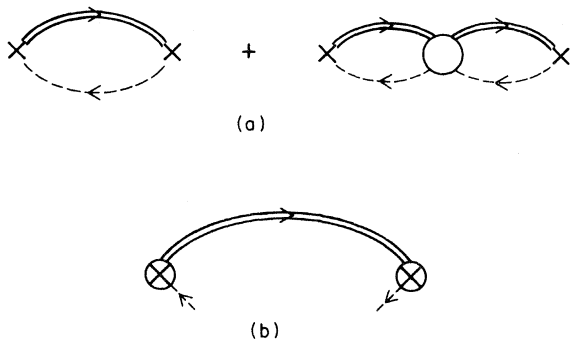


FIG. 4. (a) Diagrams contributing to the hybridization response function. The vertex denoted by the circle depends on three energy variables in this case. (b) Schematic representation of the derivative of the hybridization response function with respect to $|\omega|$.

Comparing (3.14) with (3.19) we have that $\Omega/\Lambda$ must be a constant within the leading and next-leading orders. Hence $\Omega$ and $\Lambda$ renormalize in the same way and we may set $\Omega=\Lambda$, since we have already chosen the proper proportionality constant in (3.16).

An alternative way is the following.[33] In all diagrams contributing to $F(\omega)$ there is a $d$-fermion line and a $c$-fermion line joining the two endpoints with incoming and outgoing energy $\omega$, respectively. We can bring the external energy $\omega$ to run only through this $c$-fermion line. The $c$-fermion propagator is $(\pi/2)\rho\,\mathrm{sgn}\omega$ if we neglect its energy dependence due to the hybridization. Its derivative with respect to $\omega$ is a delta function. Hence $dF(\omega)/d\omega$ corresponds to cutting this $c$-fermion line once at all possible parts. This corresponds to replacement of the bare two-leg vertices at the endpoints by dressed ones. Since the cut suppresses one integration loop, a dressed impurity propagator, $G_d(\omega)$ [Eq. (3.1)] appears as a multiplicative factor. It can be seen that interferences between the two two-leg vertices are nonlogarithmical in leading and next-leading order. $dF(\omega)/d|\omega|$ is schematically shown in Fig. 4(b). Hence we have

$$\frac{dF(\omega)}{d|\omega|}=-\frac{\Omega(\omega)}{|\omega|+\Omega(\omega)} \tag{3.20}$$

in agreement with (3.18) and (3.19). We make use of this result in Sec. V.

## IV. MULTIPLICATIVE RENORMALIZATION

We relate here the above results with the scaling properties of the system; i.e., we show that they are equivalent to multiplicative renormalization.

The idea of renormalization consists in eliminating successively, degrees of freedom of the system by scaling the ultraviolet cutoff $D$. When $D$ is reduced to a smaller value $D'$ we have to readjust all other parameters in order to keep the system invariant. Multiplicative renormalization is defined by the following transformation[34]:

$$\begin{aligned} &d\to z_1 d\ , \\ &\Gamma\to z_2^{-1}\Gamma,\ \ \gamma\to z_2 z_1^{-1}\gamma\ , \\ &V\to z_3^{-1}V,\ \ J_\perp^2\to z_3^2 z_1^{-1}J_\perp^2\ , \end{aligned} \tag{4.1}$$

where $\gamma$ and $J_\perp$ are the invariant couplings. The transformation should preserve the analytic dependence of the physical quantities on the energy variables. Consequently the multiplicative factors $z_i$

are only a function of $D/D'$ and the coupling constants, but do not depend on the energy variable $\omega$. It follows from the condition of multiplicative renormalization for a quantity $A$ that the Lie differential equation

$$\frac{\partial}{\partial x}\ln A[x;\gamma,J_\perp] = \frac{1}{x}\frac{\partial}{\partial \xi}\ln A[\xi;\gamma'(x;\gamma,J_\perp),J'_\perp(x;\gamma,J_\perp)]\Big|_{\xi=1} \quad (4.2)$$

is satisfied with the initial condition

$$A[1;\gamma,J_\perp]=1 . \quad (4.3)$$

Here $x=\omega/D$ and $\gamma',J'_\perp$ are the renormalized invariant couplings.

The prescription for the use of the renormalization group equation is then to calculate the perturbation expansion for a given quantity $A$ and insert this into the rhs of Eq. (4.2). The differential equation then extends the input skeleton diagrams consistently to all orders of perturbation. The perturbation expansion for $\gamma'$ and $J'_\perp$ is obtained[32] via (4.1) from the expansion of $d$, $\Gamma$, and $V$:

$$\gamma'=\gamma\frac{d(D'/D;\gamma,J_\perp)}{d(1;\gamma',J'_\perp)}\frac{\Gamma(D'/D;\gamma,J_\perp)}{\Gamma(1;\gamma',J'_\perp)} \quad (4.4)$$

and

$$(J'_\perp)^2=J_\perp^2\frac{d(D'/D;\gamma,J_\perp)}{d(1;\gamma',J'_\perp)}\left[\frac{V(D'/D;\gamma,J_\perp)}{V(1;\gamma',J'_\perp)}\right]^2 = J_\perp^2\frac{\Lambda(D'/D;\gamma,J_\perp)}{\Lambda(1;\gamma',J'_\perp)} . \quad (4,5)$$

Here $\Lambda$ is the function defined by (3.18).

In order to show the equivalence of this method with the diagramatic analysis, we rederive some of the results. The perturbation expansion up to second order for the vertices, self-energy, and the invariant couplings is given by (logarithmic approximation)

$$\Gamma\simeq 1+(\gamma\rho)^2\int_{|\omega|}^{D}d\omega'\frac{1}{\omega'+\Delta} , \quad (4.6)$$

$$V\simeq\frac{J_\perp}{2}\left[1-\gamma\rho\int_{|\omega|}^{D}d\omega'\frac{1}{\omega'+\Delta}\right] , \quad (4.7)$$

$$d\simeq 1-(\gamma\rho)^2\int_{|\omega|}^{D}d\omega'\frac{1}{\omega'+\Delta} , \quad (4.8)$$

$$\gamma'\simeq\gamma+\gamma O(\gamma\rho)^3 , \quad (4.9)$$

$$\frac{J'_\perp}{J_\perp}\simeq 1-\gamma\rho\left[1+\frac{\gamma\rho}{2}\right]\int_{|\omega|}^{D}d\omega'\frac{1}{\omega'+\Delta} . \quad (4.10)$$

It follows immediately that $\gamma'=\gamma$, i.e., $\gamma'$ is not renormalized. The Lie equation for $\Gamma$ yields

$$\frac{d\ln\Gamma(\omega)}{d|\omega|}=-(\gamma\rho)^2\frac{1}{|\omega|+\Omega(\omega)} \quad (4.11)$$

which is equivalent to (3.7) if $\Gamma(\omega)d(\omega)$ is replaced by one. Similarly we obtain

$$\frac{d\ln V(\omega)}{d|\omega|}=\gamma\rho\frac{1}{|\omega|+\Omega(\omega)} , \quad (4.12)$$

$$\frac{d\ln d(\omega)}{d|\omega|}=(\gamma\rho)^2\frac{1}{|\omega|+\Omega(\omega)} , \quad (4.13)$$

and

$$\frac{d\ln J'_\perp}{d|\omega|}=\gamma\rho\left[1+\frac{\gamma\rho}{2}\right]\frac{1}{|\omega+\Omega(\omega)} . \quad (4.14)$$

The square of $J'_\perp$ transforms like $\Omega(\omega)$. Herewith we reproduced equations (3.13), (3.10), and (3.14).

For the sake of completeness we also reproduce Eq. (3.19). The perturbation expansion for the response function $F(\omega)$ is given by (logarithmic approximation)

$$F(\omega)=\frac{\pi}{4}J_\perp^2\rho\int_{|\omega|}^{D}d\omega'\frac{1}{\omega'+\Delta}\times\left[1-\gamma\rho\int_{|\omega|}^{D}d\omega''\frac{1}{\omega''+\Delta}-(\gamma\rho)^2\ln\frac{D}{|\omega'|+\Delta}+\ldots\right] . \quad (4.15)$$

Here we included only the relevant skeleton diagrams. Taking the derivative with respect to $|\omega|$ we obtain the perturbation expansion for

$$\Lambda=1-2\gamma\rho\int_{|\omega|}^{D}d\omega'\frac{1}{\omega'+\Delta}-(\gamma\rho)^2\ln\frac{D}{|\omega|+\Delta} . \quad (4.16)$$

Since $\Lambda$ obeys multiplicative renormalization it satisfies the following Lie equation:

$$\frac{d\ln\Lambda(\omega)}{d|\omega|}=2\gamma\rho(1+\tfrac{1}{2}\gamma\rho)\frac{1}{|\omega|+\Omega(\omega)} . \quad (4.17)$$

This result is in agreement with (4.14).

In the limit $V\to 0$ Eqs. (4.9), (4.11)–(4.13), and (4.17) are the scaling equations for the corresponding quantities in the x-ray-threshold problem.[34] Hence we may obtain the scaling equations of our resonant level model, Eq. (2.7), by replacing the dynamical variable $|\omega|$ by $|\omega|+\Omega$ in the rhs of the Lie equations for the x-ray-threshold problem. The result is then correct for small $J_\perp\rho$. We are

going to assume that this rule is also valid if $\gamma\rho$ is not small. In this way the x-ray-threshold solution provides a useful tool to calculate, e.g., $\Omega(\omega)$ within the same approximation as our transformation of the model in Sec. II (long-time limit) and to obtain an accurate extrapolation to $\gamma\rho\simeq\sqrt{2}-1$. We restrict ourselves to small $J_\perp\rho$.

## V. THE X-RAY THRESHOLD ANALOGY

Our transformed Hamiltonian [Eq. (2.7)] for $J_\perp=0$ corresponds to the x-ray-threshold problem. This problem has been solved by Nozières and de Dominicis[35] in the long-time approximation. The x-ray absorption and emission spectrum can also be obtained for nonzero temperature. We require our Kondo solution to contain the x-ray problem as a limit for all temperatures. It provides us an aid to extend the results of the preceding section to $T\neq 0$ and to fix multiplicative constants which cannot be obtained from the renormalization procedure.

This section is organized as follows. We first obtain the x-ray absorption and emission spectrum for $T=0$ from the scaling equations of Secs. III and IV, then we give the finite-temperature solution using the bosonization technique,[36] and finally we combine the results in order to obtain the resonance width self-consistently and for all temperatures.

### A. The x-ray-threshold spectrum at $T=0$

In the x-ray-absorption process the incoming photon excites a deep-lying core electron into the conduction band. Electron-hole excitations with arbitrarily low energy are generated in the electron gas during the absorption process. These electron-hole excitations give rise to logarithmical divergences in the absorption spectrum. Neglecting the momentum dependence of the scattering potential, the Hamiltonian of the x-ray-threshold problem can be written as

$$H_{\rm xray}=\sum_{\vec{k}}\epsilon_k c^\dagger_{\vec{k}}c_{\vec{k}}-Vd^\dagger d\sum_{\vec{k}\,\vec{k}'}c^\dagger_{\vec{k}}c_{\vec{k}'}+Ed^\dagger d\ , \tag{5.1}$$

where $V$ is the strength of the scattering potential and $d^\dagger d$ the occupation number of the deep core level. This is just our transformed Hamiltonian (2.7) with $V=\gamma$, $E=-B$, and $J_\perp=0$. The dipole operator should annihilate the deep core electron and create a conduction electron, such that the absorption and emission spectrum are given by the dissipative part of the correlation function

$$\langle\langle c^\dagger d;d^\dagger c\rangle\rangle_\omega\ . \tag{5.2}$$

This is essentially the hybridization response function denoted by $F(\omega)$ in the preceding section. In other words, the solution of the x-ray problem provides us the exact $F(\omega)$ in second order in $J_\perp$.

The x-ray-threshold problem has been solved by many methods. Roulet *et al.*[30] used the parquet formalism to obtain the absorption spectrum, Nozières and de Dominicis[35] reduced the problem to a one-body scattering solved by the Muskhelishvili method, Schotte[36] used the technique of bosonizing fermions, and Sólyom[34] applied the renormalization group.

The one-body aspect of the problem is due to the fact that the number of core electrons is a conserved quantity for $H_{\rm x\ ray}$. This leads to the Ward identity[24]

$$\Gamma(\omega,\omega-\omega';\omega')=\frac{1}{i\omega'}[G_d^{-1}(\omega)-G_d^{-1}(\omega-\omega')]\ , \tag{5.3}$$

where $\Gamma$ is the vertex associated with the scattering potential $V$, $G_d$ is the core-electron propagator, and $\omega$ and $\omega-\omega'$ are the energies of the incoming and outgoing $d$ particles. With the aid of (5.3) one can derive an integral equation for $G_d$ which leads to the solution of the problem.

The zero-temperature solution can also be obtained from (4.17) by setting $\Omega=0$ and $V=\gamma$:

$$\Lambda(\omega)=A(|\omega|/D)^{2\gamma\rho+(\gamma\rho)^2}\ , \tag{5.4}$$

where $A$ is a constant which tends to one when $\gamma\rho\to 0$. This is the asymptotically exact solution for $\omega\to 0$. The function $F(\omega)$ is obtained by integrating (5.4) once more with respect to $\omega$. Then we have to regularize the function, and its cut on the real-energy axis yields the x-ray emission and absorption spectrum. If $\gamma<0$, the spectrum diverges at the threshold, whereas if $\gamma>0$, which is the case of our interest, the function vanishes at $\omega=0$.

Hence, in our case, $\Lambda$ is an increasing function of $|\omega|$. The interference of the logarithmic singularities is destructive. This is similar to what happens for ferromagnetic Kondo coupling, where higher-order corrections play a secondary role. A

more sophisticated evaluation of $\Lambda$ is needed to determine the multiplicative constant $A$ and the temperature dependence of the function. For this purpose we use the technique of bosonizing fermions.

### B. The x-ray spectrum at nonzero temperature

In the context of the x-ray-threshold problem, the bosonization technique was first used by Schotte and Schotte.[36] We return to our formulation in Sec. II, where we expressed the Hamiltonian in terms of boson operators

$$a_k^\dagger = \frac{1}{\sqrt{k}} \sum_{p=0}^{k_0} c_{p+k}^\dagger c_p \tag{5.5}$$

which represent the electron-hole excitation of the system

$$H_{\text{xray}} = \sum_{k>0} \frac{k}{\rho_F} a_k^\dagger a_k + E d^\dagger d - \gamma d^\dagger d \sum_{k>0} \sqrt{k}\,(a_k^\dagger + a_k) . \tag{5.6}$$

The correlation function (4.2) transcribed into the boson representation yields

$$\left\langle\left\langle \exp\left[\sum_{k>0} \frac{1}{\sqrt{k}}(a_k^\dagger - a_k)\right] d;\; d^\dagger \exp\left[-\sum_{k>0} \frac{1}{\sqrt{k}}(a_k^\dagger - a_k)\right]\right\rangle\right\rangle_\omega , \tag{5.7}$$

where we made use of expression similar to (2.4). The Hamiltonian (5.6) can be diagonalized by applying the transformation (2.6) with the factor $(1-\sqrt{2})$ in the exponent replaced by $\gamma\rho$. Since the correlation function remains invariant under the transformation we obtain[36]

$$\left\langle\left\langle \exp\left[(1+\gamma\rho)\sum_{k>0} \frac{1}{\sqrt{k}}(a_k^\dagger - a_k)\right] d;\; d^\dagger \exp\left[-(1+\gamma\rho)\sum_{k>0} \frac{1}{\sqrt{k}}(a_k^\dagger - a_k)\right]\right\rangle\right\rangle_\omega , \tag{5.8}$$

which is to be evaluated for a free Bose gas, since the transformed Hamiltonian reads

$$H_{\text{xray}} = \sum_{k>0} \frac{k}{\rho_F} a_k^\dagger a_k + E d^\dagger d . \tag{5.9}$$

Equation (5.8) is conveniently evaluated as a function of time[26]; for $t >> \rho_F$ one obtains

$$\left\langle \exp\left[(1+\gamma\rho_F)\sum_{k>0} \frac{1}{\sqrt{k}}[a_k^\dagger(t) - a_k(t)]\right] \exp\left[-(1+\gamma\rho_F)\sum_{k>0} \frac{1}{\sqrt{k}}[a_k^\dagger(0) - a_k(0)]\right]\right\rangle = (i\rho_F \pi T/\sinh\pi t T)^{(1+\gamma\rho_F)^2} = A(t) . \tag{5.10}$$

The restrictions to time $t$ larger than $\rho_F$ are due to the facts that the $a_k$ operators behave like bosons for small momentum only and that the momentum cutoff of the integration in (5.10) is $k_0$. In the literature this is known as the long-time approximation.[20,35]

The dissipative part of the correlation function (5.2) is given by

$$\langle\langle c^\dagger d; d^\dagger c\rangle\rangle''_\omega = -\int \frac{d\omega'}{2\pi} \chi_B''(\omega') \left[1 + \text{cotanh}\frac{\omega'}{2T} \tanh\frac{\omega-\omega'}{2T}\right] \chi_d''(\omega-\omega') , \tag{5.11}$$

where $\chi_d''$ is the imaginary part of a free fermion propagator with energy $E$,

$$\chi_d''(\omega) = \pi\delta(\omega - E) \tag{5.12}$$

and $\chi_B''$ is obtained by Fourier-transforming (5.10):

$$\chi_B''(\omega) = \int dt\, e^{i\omega t}[A(t) - A(-t)] = \rho_F \sinh\frac{\omega}{2T} \left(\frac{2\pi T}{D}\right)^{(1+\gamma\rho_F)^2 - 1} \left|\Gamma\left[\frac{1}{2}(1+\gamma\rho_F)^2 + \frac{i\omega}{2\pi T}\right]\right|^2 \Big/ \Gamma((1+\gamma\rho_F)^2) . \tag{5.13}$$

Here we used $\rho_F = 1/D$. The function $\chi_B''(\omega)$ is the discontinuity of $\chi_B(z)$ along the real-energy axis. The function $\chi_B(z)$ is obtained by continuating analytically (5.13) into the complex energy plane

$$\chi_B(z)=\frac{1}{\pi T}\sin\left[\frac{\pi}{2}(1+\gamma\rho_F)^2\right]\left[\frac{2\pi T}{D}\right]^{(1+\gamma\rho_F)^2}B_x\left[\tfrac{1}{2}(1+\gamma\rho_F)^2-i\frac{z}{2\pi T},1-(1+\gamma\rho_F)^2\right], \tag{5.14}$$

where $B_x$ is the incomplete beta function and $x=\exp(-2\pi T/D)$. We have, finally, that for $E=0$,

$$\langle\langle c^\dagger d;d^\dagger c\rangle\rangle_z=-\tfrac{1}{2}\chi_B(z)\ . \tag{5.15}$$

We now discuss two important limits of (5.15): The cases when $\gamma\to 0$ and when $\gamma\rho_F\to(\sqrt{2}-1)$. The latter case corresponds to $J_{||}\rho\to 0$ in Eq. (2.7). If $\gamma\to 0$, we obtain from (5.14)

$$\langle\langle c^\dagger d;d^\dagger c\rangle\rangle_z=-\frac{1}{D}\left[\ln\frac{D}{2\pi T}-\psi\left[\frac{1}{2}-i\frac{z}{2\pi T}\right]\right]\quad(\gamma\to 0) \tag{5.16}$$

such that

$$\langle\langle c^\dagger d;d^\dagger c\rangle\rangle''_\omega=-\frac{\pi}{2}\rho_F\tanh\frac{\omega}{2T}\ . \tag{5.17}$$

Here $\psi$ is the digamma function. This corresponds to the free bubble, Eq. (3.17), calculated for nonzero temperature and $\Omega=0$. For small $\gamma\rho_F$ we obtain from (5.14)

$$\langle\langle c^\dagger d;d^\dagger c\rangle\rangle_z=-\rho_F\frac{1}{1-(1+\gamma\rho_F)^2}\left[\exp\left\{[1-(1+\gamma\rho_F)^2]\left[\ln\frac{D}{2\pi T}-\psi\left[\frac{1}{2}-i\frac{z}{2\pi T}\right]\right]\right\}-1\right]. \tag{5.18}$$

The derivative of this expression with respect to the free bubble shows the power-law behavior found in (5.4), now extended to $T\neq 0$.

The second case of interest is when $\gamma\rho_F=\sqrt{2}-1-J_{||}\rho_F/\sqrt{2}$. We have then

$$\langle\langle c^\dagger d;d^\dagger c\rangle\rangle_z=\frac{\pi}{2}\rho_F^2\frac{\Gamma(1+2\epsilon)}{(1-2\epsilon)}(2\pi T\epsilon-iz)\exp\left\{2\epsilon\left[\ln\frac{D}{2\pi T}-\psi\left[1-i\frac{z}{2\pi T}\right]\right]\right\}, \tag{5.19}$$

where $\epsilon=J_{||}\rho-\frac{1}{4}(J_{||}\rho)^2$ is supposed to be small. The last factor yields a power-law behavior similar to that of (5.18). In the limit $\epsilon\to 0$ we obtain

$$\langle\langle c^\dagger d;d^\dagger c\rangle\rangle_z=-i\frac{\pi}{2}\rho_F^2 z\ . \tag{5.20}$$

The linear dependence on the energy stems from the electron-hole excitations in the Fermi sea of the Kondo problem.

At $T=0$ and for small $\gamma\rho$ the function $\Lambda(\omega)$ is obtained by differentiating $\langle\langle c^\dagger d;d^\dagger c\rangle\rangle_\omega$ with respect to $\ln(D/|\omega|)$ [Eq. (3.18)]. The generalization to $T\neq 0$ is to differentiate $\langle\langle c^\dagger d;d^\dagger c\rangle\rangle_\omega$ with respect to (5.16), i.e., the bare correlation function ($\gamma=0$). This procedure is not well defined when $\gamma\rho\simeq\sqrt{2}-1$, since it is hard to express (5.19) in terms of the bare correlation. An alternative procedure is to calculate $\Lambda$ from the anticommutator correlation function $\langle\langle c^\dagger d;\ d^\dagger c\rangle\rangle^\dagger_\omega$, as seen below.

### C. Renormalization of the resonance width for $J_\perp\to 0$

The dissipative parts of the commutator and anticommutator functions are related by the fluctuation-dissipation theorem, such that in (5.13) the $\sinh(\omega/2T)$ must be replaced by $\cosh(\omega/2T)$. The analytical continuation into the complex energy plane replaces the sin in (5.14) by cos; hence we have

$$\chi_B^+(z)=i\cot an\left[\frac{\pi}{2}(1+\gamma\rho_F)^2\right]\chi_B(z)+g(z)\ , \tag{5.21}$$

where $g(z)$ is a regular function (no singularities on the real axis) and

$$\langle\langle c^\dagger d;d^\dagger c\rangle\rangle^\dagger_z=-\tfrac{1}{2}\chi_B^+(z)\ . \tag{5.22}$$

For small $\gamma\rho$ we obtain

$$\langle\langle c^\dagger d;d^\dagger c\rangle\rangle^\dagger_z=-\frac{i\pi}{2D}\exp\left\{[1-(+\gamma\rho_F)^2]\times\left[\ln\frac{D}{2\pi T}-\psi\left[\frac{1}{2}-i\frac{z}{2\pi T}\right]\right]\right\} \tag{5.23}$$

which reduces to the constant $-i\pi/2D$ for $V\to 0$. This expression is just $(i\pi)$ times the derivative of (5.18) with respect to the bare correlation (5.16). Hence (5.23) is proportional to $\Lambda$ for small $\gamma\rho_F$ and we have

$$\Omega(z)=\Lambda(z)=\frac{i}{2}J_\perp^2\langle\langle c^\dagger d;d^\dagger c\rangle\rangle_z^\dagger \tag{5.24}$$

in the limit $J_\perp\rho\to 0$. Since we calculated $\chi_B(z)$ within the same approximation as the transformation procedure of Sec. II, the validity of (5.24) also extends to coupling strength $\gamma\rho$ of the order of $\sqrt{2}-1$. For small $J_\perp\rho$ the above expression reduces to

$$\Omega(z)=\tfrac{1}{2}(J_\perp\rho_F)^2\left[\pi T\exp[2\epsilon\phi(z)]-\frac{iz}{2\epsilon}\{\exp[2\epsilon\phi(z)]-1\}\right], \tag{5.25}$$

where

$$\phi(z)=\ln\frac{D}{2\pi T}-\psi\left[1-i\frac{z}{2\pi T}\right]. \tag{5.26}$$

Equation (5.25) is the extension of (5.4) to nonzero temperature. In the limit $T\to 0$ we obtain the multiplicative constant $A=1/\pi J_{||}\rho_F$ by comparing the nonanalytic terms for $z\leftrightarrow i\,|\omega|$. It should be mentioned that our application of the renormalization group in Sec. IV does not generate analytic terms in $z$.

The above result for $\Omega(z)$ can be written as

$$\Omega(z)=\tfrac{1}{2}(\pi TA[\phi]-izB[\phi]), \tag{5.27}$$

where $A$ and $B$ satify the relation

$$\frac{d}{d\phi}B[\phi]=A[\phi]. \tag{5.28}$$

This relation is the necessary and sufficient condition to obtain the Fermi-liquid behavior at low temperatures when we include the resonance width. This is seen later in the third paper. The function $A[\phi]$ gives rise to the renormalized Korringa relaxation rate and $B[\phi]$ to the renormalization of the static susceptibility. In this way (5.28) underlines the close relation between the dynamics of the impurity spin and its static susceptibility.

The function $g(z)$ in (5.21) is still not determined. Since it is a regular function it does not contribute with logarithmic singularities to (5.25), but it may cause a shift in $\Omega(z)$. The $g(z)$ is determined from the condition of multiplicative renormalizability for $A[\phi]$ and $B[\phi]$. There is then an additive constant to $B$ of $(J_\perp\rho)^2/2\epsilon$ such that

$$B[\phi]=\frac{(J_\perp\rho)^2}{2\epsilon}\exp[2\epsilon\phi(z)]. \tag{5.29}$$

Note that the relation (5.28) is not modified by an additive constant to $B$. As will be seen in the following papers, this additive constant represents the polarization of the conduction electrons on the impurity; i.e., the Knight shift. In a system with full-spin rotational invariance the additive constant is $J\rho$.

### D. Scaling equation for the resonance width for $T\neq 0$

We now relate Eq. (5.27) with the scaling equation for $\Omega$ obtained in Secs. III and IV in order to incorporate $\Omega$ in the rhs of (5.27). We make use of the rule stated at the end of Sec. IV by which the scaling variable $|\omega|$ is to be replaced by $|\omega|+\Omega$ on the rhs of the scaling equation.

Let us first consider (5.27) in the zero-temperature limit. We set $z=i\,|\omega|$ and differentiate with respect to $|\omega|$:

$$\frac{d\Omega}{d|\omega|}=\tfrac{1}{2}(B-A)=\tfrac{1}{2}(1-2\epsilon)B=(1-2\epsilon)\frac{\Omega}{|\omega|}, \tag{5.30}$$

which is just (3.14) if we replace $|\omega|$ by $|\omega|+\Omega$. Differentiating (5.27) for $T\neq 0$ we obtain

$$\frac{d\Omega}{d|\omega|}=\frac{1}{2}\left[B[\phi]+\left[\pi T\frac{dA}{d\phi}+|\omega|\frac{dB}{d\phi}\right]\frac{d\phi}{d|\omega|}\right], \tag{5.31}$$

where

$$\frac{d\phi}{d|\omega|}=-\frac{1}{2\pi T}\psi'\left[1+\frac{|\omega|}{2\pi T}\right]. \tag{5.32}$$

Replacing now $|\omega|$ by $|\omega|+\Omega$ according to the above rule we obtain

$$\frac{d\Omega}{d|\omega|}=\frac{1}{2}\left[B[\phi]-\left[\pi T\frac{dA}{d\phi}+(|\omega|+\Omega)A[\phi]\right]\times\frac{1}{2\pi T}\psi'\left[1+\frac{|\omega|+\Omega}{2\pi T}\right]\right], \tag{5.33}$$

with

$$\phi(\omega)=\ln\frac{D}{2\pi T}-\psi\left[1+\frac{|\omega|+\Omega}{2\pi T}\right]. \quad (5.34)$$

In the limit $T\to 0$ we recover (3.14). Expression (5.33) is then the merging of the zero-temperature results with linewidth and the temperature-dependent result without hybridization.

## VI. SUMMARY AND DISCUSSION

The crossover from thermal relaxation at high temperatures to an inherent relaxation of the spin in the singlet state represents a symmetry breaking which cannot be achieved by ordinary perturbation theory. In order to start with a finite lifetime we transformed the system, making use of the boson transcription of fermions, such that we have a resonance level (Toulouse limit[17–20]) and a large perturbation $\gamma$. This transformation is asymptotically exact within the long-time approximation. The perturbation expansion with respect to $\gamma$ still yields logarithmic contributions, but the resonance width of the virtual bound state now plays the role of an infrared cutoff. The perturbation expansion is no longer divergent term by term. Moreover, it is seen that the resonance width is reduced by the renormalization if $\gamma$ is positive. This means, in other words, that the interference of the logarithmic contributions is destructive, similar to what happens for the perturbation theory in $J$ for ferromagnetic coupling. In this way a good convergence of the perturbation series is guaranteed.

In Secs. III and IV we showed that the transformed model renormalizes multiplicatively in leading and next-leading logarithmic order. A comparison with the scaling equations of the x-ray-threshold problem shows that the scaling equations of our model (2.7) can be obtained from those of the x-ray problem by replacing the dynamical variable $|\omega|$ by $|\omega|+\Omega$ on the rhs of the Lie differential equations (Sec. IV).

The renormalization group yields the renormalized quantities up to a multiplicative constant. For $J_\perp=0$ our model corresponds to the Hamiltonian of the x-ray-threshold problem. We used this analogy to the x-ray-threshold problem to determine the multiplicative constants by requiring that the x-ray-threshold solution is reproduced for vanishing resonance width. The x-ray-threshold spectrum is asymptotically exactly known for long times and as a function of temperature. The temperature dependence of the x-ray problem allowed us to extend the zero-temperature results to nonzero temperatures. The main result is the renormalization equation (5.33) for the resonance width. The relation (5.28) is the condition for the Fermi-liquid properties of the system (paper III).

In order to calculate properties of the Kondo system we have to integrate Eq. (5.33). In the following paper we present a simplified solution in which the energy dependence of $\Omega$ is neglected under the integral. In this way we obtain a transcendental equation which can be solved for the interesting limits. This simplified solution already provides a qualitative correct Kondo susceptibility. It interpolates between the asymptotic freedom and infrared slavery, yielding a smooth crossover. At high temperatures the theory reproduces correctly the lower-order perturbation theory, and at low temperatures the susceptibility and the relaxation time remain finite (indicating the singlet ground state) and vary with temperature according to a Fermi-liquid theory.

Owing to the preferential treatment of $J_{||}$ with respect to $J_\perp$, this approximation scheme breaks the spin-rotational invariance. This drawback is discussed and corrected in paper III. The modification of the theory is along the following line. For $\gamma\rho\simeq\sqrt{2}-1$ there are additional logarithmic contributions to the four-leg vertex $\Gamma$, such that the invariant coupling $\gamma$, i.e., $J_{||}$, is renormalized and no longer equal to its bare value. A consequent reconsideration of the logarithmic contributions eventually leads to the spin-rotational invariance of the system.

It should be mentioned that Filyov and Wiegmann[37] applied the Bethe ansatz to the Hamiltonian (2.7). The fact that the wave function factorizes into a product of two-body wave functions seems to reflect in the simple structure of the renormalization-group equations derived here, as well as in numerous Ward cancellations.

[1] J. Kondo, in *Solid State Physics*, edited by F. Seitz, D. Turnbull, and H. Ehrenreich (Academic, New York, 1969), Vol. 23, p. 183.

[2] *Magnetism*, edited by H. Suhl (Academic, New York, 1973), Vol V.

[3] P. Nozières, in *Proceedings of LT 14*, edited by M. Krusius and M. Vuorio (North-Holland, Amsterdam, 1975), Vol. 5, p. 339.

[4]K. G. Wilson, Rev. Mod. Phys. 47, 773 (1975).
[5]P. Steiner, W. v. Zdrojewski, D. Gumprecht, and S. Hüfner, Phys. Rev. Lett. 31, 355 (1973).
[6]M. Loewenhaupt and W. Just, Phys. Lett. 53A, 305 (1975).
[7]H. Alloul, Physica (Utrecht) 86–88B, 449 (1977).
[8]J. L. Tholence and R. Tournier, Phys. Rev. Lett. 25, 867 (1970).
[9]W. M. Star, F. B. Basters, G. M. Nap, E. De Vroede, and C. van Baarle, Physica (Utrecht) 58, 585 (1972).
[10]A. A. Abrikosov and A. A. Migdal, J. Low Temp. Phys. 3, 519 (1970).
[11]P. B. Vigman, Zh. Eksp. Teor. Fiz. Pis'ma Red. 31, 392 (1980) [JETP Lett. 31, 364 (1980)].
[12]N. Andrei, Phys. Rev. Lett. 45, 379 (1980).
[13]V. M. Filyov, A. M. Tzvelik, and P. B. Wiegmann, Phys. Lett. 81A, 175 (1981).
[14]N. Andrei and J. H. Lowenstein, Phys. Rev. Lett. 46, 356 (1981).
[15]W. Götze and P. Schlottmann, Solid State Commun. 13, 17 (1973).
[16]W. Götze and P. Schlottmann, J. Low Temp. Phys. 16, 87 (1974).
[17]P. Schlottmann, J. Magn. Magn. Mater. 7, 72 (1978).
[18]P. Schlottmann, J. Phys. (Paris) 39, C6–1486 (1978).
[19]G. Toulouse, C. R. Acad. Sci. 268, 1200 (1969).
[20]P. W. Anderson, G. Yuval, and D. R. Hamann, Phys. Rev. B 1, 4464 (1970).
[21]P. Noxières, J. Low Temp. Phys. 17, 31 (1974).
[22]K. Yamada, Prog. Theor. Phys. 53, 970 (1975).
[23]K. D. Schotte and U. Schotte, Phys. Rev. B 4, 2228 (1971).
[24]P. Schlottmann, Phys. Rev. B 22, 622 (1980).
[25]S. Tomonaga, Prog. Theor. Phys. 5, 544 (1950); J. M. Luttinger, J. Math. Phys. 4, 1154 (1963).
[26]K. D. Schotte, Z. Phys. 230, 99 (1970).
[27]P. B. Vigman and A. M. Finkel'stein, Zh. Eksp. Teor. Fiz. 75, 204 (1978) [Sov. Phys.—JETP 48, 102 (1978)].
[28]V. V. Sudakov, Dokl. Akad. Nauk SSSR 111, 338 (1956) [Sov. Phys.—Dokl. 1, 662 (1956)].
[29]A. A. Abrikosov, Physics (N.Y.) 2, 5 (1965).
[30]B. Roulet, J. Gavoret, and P. Nozières, Phys. Rev. 178, 1072 (1969).
[31]R. Gerhardts and P. Schlottmann, Z. Phys. B 34, 349 (1979).
[32]P. Schlottmann, Phys. Rev. B 22, 613 (1980).
[33]H. Shiba, Prog. Theor. Phys. 54, 967 (1975).
[34]J. Sólyom, J. Phys. F 4, 2269 (1974).
[35]P. Nozières and C. T. de Dominicis, Phys. Rev. 178, 1097 (1969).
[36]K. D. Schotte and U. Schotte, Phys. Rev. 182, 479 (1969).
[37]V. M. Filyov and P. B. Wiegmann, Phys. Lett. 76A, 283 (1980).